Global DNA methylation analysis reveals miR-214-3p contributes to cisplatin resistance in pediatric intracranial nongerminomatous malignant germ cell tumors

Tsung-Han Hsieh,[§] Yun-Ru Liu,[§] Ting-Yu Chang, Muh-Lii Liang, Hsin-Hung Chen, Hsei-Wei Wang, Yun Yen, and Tai-Tong Wong

Joint Biobank, Office of Human Research, Taipei Medical University, Taipei, Taiwan (T-H.H., Y-R.L.); Comprehensive Cancer Center of Taipei Medical University, Taipei Medical University, Taipei, Taiwan (T-H.H., Y-R.L., T-Y.C., Y.Y., T-T.W.); Research Center of Cancer Translational Medicine, Taipei Medical University, Taipei, Taiwan (T-H.H., T-Y.C.); Division of Pediatric Neurosurgery, Neurological Institute, Taipei Veterans General Hospital (VGH-TPE), Taipei, Taiwan (M-L.L., H-H.C.); Institute of Microbiology and Immunology, National Yang-Ming University, Taipei, Taiwan (H-W.W.); Program for Cancer Biology and Drug Discovery, College of Medical Science and Technology, Taipei Medical University, Taipei, Taiwan (Y.Y.); Institutes of Clinical Medicine, Taipei Medical University, Taipei, Taiwan (T-T.W.); Department of Neurosurgery, Taipei Medical University Hospital, Taipei Medical University, Taipei, Taiwan (T-T.W.); Neuroscience Research Center, Taipei Medical University Hospital, Taipei, Taiwan (T-T.W.)

Corresponding Authors: Tai-Tong Wong, Department of Neurosurgery, Taipei Medical University Hospital, Taipei Medical University, Taipei, Taiwan. Address: No.250, Wuxing St., Xinyi Dist., Taipei City 110, Taiwan (R.O.C.) (ttwong99@gmail.com) and Yun Yen, Program for Cancer Biology and Drug Discovery, College of Medical Science and Technology, Taipei Medical University, Taipei, Taiwan. Address: No.250, Wuxing St., Xinyi Dist., Taipei City 110, Taiwan (R.O.C.) (yyen@tmu.edu.tw).

§These authors contributed equally to this work.

Abstract

Background. Pediatric central nervous system germ cell tumors (CNSGCTs) are rare and heterogeneous neoplasms, which can be divided into germinomas and nongerminomatous germ cell tumors (NGGCTs). NGGCTs are further subdivided into mature teratomas and nongerminomatous malignant GCTs (NGMGCTs). Clinical outcomes suggest that NGMGCTs have poor prognosis and survival and that they require more extensive radiotherapy and adjuvant chemotherapy. However, the mechanisms underlying this difference are still unclear. DNA methylation alteration is generally acknowledged to cause therapeutic resistance in cancers. We hypothesized that the pediatric NGMGCTs exhibit a different genome-wide DNA methylation pattern, which is involved in the mechanism of its therapeutic resistance.

Methods. We performed methylation and hydroxymethylation DNA immunoprecipitation sequencing, mRNA expression microarray, and small RNA sequencing (smRNA-seq) to determine methylation-regulated genes, including microRNAs (miRNAs).

Results. The expression levels of 97 genes and 8 miRNAs were correlated with promoter DNA methylation and hydroxymethylation status, such as the miR-199/-214 cluster, and treatment with DNA demethylating agent 5-aza-2'-deoxycytidine elevated its expression level. Furthermore, smRNA-seq analysis showed 27 novel miRNA candidates with differential expression between germinomas and NGMGCTs. Overexpresssion of miR-214-3p in NCCIT cells leads to reduced expression of the pro-apoptotic protein BCL2-like 11 and induces cisplatin resistance.

Conclusions. We interrogated the differential DNA methylation patterns between germinomas and NGMGCTs and proposed a mechanism for chemoresistance in NGMGCTs. In addition, our sequencing data provide a roadmap for further pediatric CNSGCT research and potential targets for the development of new therapeutic strategies.

Key words

CNSGCTs | DNA methylation | miR-214-3p | NGMGCTs | therapeutic resistance

Importance of the study

NGMGCTs are malignant pediatric brain tumors, which have a poorer prognosis than germinomas. However, few studies have discussed this phenomenon. We employed methylation and hydroxymethylation DNA immunoprecipitation sequencing and identified a mechanism that contributed to the chemotherapy resistance in NGMGCTs. Furthermore, our findings not only provide insights into the possible molecular mechanisms underlying the therapeutic resistance of NGMGCTs but also provide clues that may help in the development of new target therapies and therapeutic strategies in the future.

Central nervous system germ cell tumors (CNSGCTs) are rare and heterogeneous. Their incidence varies significantly according to geography. CNSGCTs constitute 3% of tumors in Western countries compared with 11%–15% of all pediatric CNS tumors observed in Japan, Korea, and Taiwan. The histological types of CNSGCTs are germinomas and nongerminomatous GCTs (NGGCTs).[1] NGGCTs are further subdivided into mature teratomas and nongerminomatous malignant GCTs (NGMGCT), including immature teratomas, teratomas with malignant transformation, yolk sac tumors, embryonal carcinomas, choriocarcinomas, and mixed GCTs. Common locations for the development of CNSGCTs are the pineal gland, sellar region, basal ganglia, and ventricles.[2] The diagnosis is made based on the clinical features, neuroimaging findings, serum tumor marker levels (alpha-fetaprotein and beta human chorionic gonadotropin), histological findings, and response to radiation therapy and/or chemotherapy in selective patients. A histopathological comparison of the degrees of differentiation and malignancy of NGMGCTs indicates that germinomas are the most undifferentiated GCT. Germinomas and NGMGCTs carry different prognoses and sensitivities to chemotherapy and radiotherapy.[3] Germinomas also show a good response to dose reduction in extended focal radiation therapy and a good prognosis with or without less intensive chemotherapy.[4] However, NGMGCTs require not only standard dose radiotherapy but also intensive chemotherapy[5]; furthermore the outcomes are markedly worse than those of germinomas. The mechanisms underlying this chemotherapy-related difference between NGMGCTs and germinomas are still unclear.

DNA methylation at the fifth position of cytosine (5mC) is an important epigenetic modification of the mammalian genome that is involved in the regulation of many biological processes, including embryonic development, gene and microRNA transcription, cellular differentiation, X chromosome inactivation, genomic imprinting, and chromosome instability.[6] Accordingly, 5mC has long been considered a stable epigenetic marker of DNA. In 2009, ten-eleven-translocation (TET) family dioxygenases were identified, which can oxidize 5mC to intermediate products, including 5-hydroxymethylcytosine (5hmC), 5-formylcytosine (5fC), and 5-carboxylcytosine (5caC).[7] Aberrant 5mC and 5hmC expression patterns are associated with tumor formation.[8–10] Hypermethylation at specific promoter regions of tumor suppressor genes, such as DNA repair pathway genes (*hMLH1*, *MGMT*, and *BRCA1*), cell cycle control genes (*p16^{ink4a}*, *p15^{ink4b}*, and *RB*), apoptotic or proapoptotic proteins (*APAF-1* and *DAPK1*), and p53 network genes (*p14^{ARF}*, *p73*, and *SFRP1*), has been associated with

drug resistance.[10,11] However, the mechanisms of methylation-regulated coding and noncoding genes that cause chemotherapy resistance in NGMGCTs are still unclear.

MicroRNAs (miRNAs) are 21- to 23-nucleotide (nt), single-strand, noncoding RNAs that play essential roles in many cellular processes, including development, stem cell division, differentiation, apoptosis, disease, and cancer formation.[12] Many studies have distinguished between the global miRNA profiles of germinomas and NGMGCTs.[13,14] Wang et al reported that some miRNAs, such as miR-142-5p, were downregulated in NGMGCTs and some, such as miR-335 and miR-654-3p, were upregulated.[13] Palmer et al indicated that the miR-371–373 and miR-302 clusters were upregulated in malignant GCTs.[14]

In the present study, we performed methylation and hydroxymethylation DNA immunoprecipitation sequencing (MeDIP-seq and hMeDIP-seq, respectively) to analyze the differential DNA methylation and hydroxymethylation signatures between germinomas and NGMGCTs. We identified several genes and miRNAs, such as *FZD7* and the miR-199a/-214 cluster, that were hypomethylated and upregulated in NGMGCTs. Furthermore, we demonstrated that in NGMGCTs, miR-214-3p overexpression enhanced cisplatin resistance by downregulating the expression of its target, the apoptotic protein BCL2-like 11 (BCL2L11/BIM).

Materials and Methods

Biological Samples

The parent/legal guardian of the patients in this study provided informed consent, and all procedures were approved by the institutional review board of VGH-TPE (VGHIRBNU.:20I004018IA). Fresh-frozen tumor tissues were collected during surgery from patients with intracranial GCTs. Data of the study cases were retrieved from the surgical pathology files of the Department of Pathology and Laboratory Medicine at Taipei Veterans General Hospital.

Cell Culture

Human embryonic kidney (HEK)293T cells were obtained from the American Type Culture Collection. Human embryonal carcinoma NCCIT cells were obtained from Dr Huang's lab (Taipei Medical University, Taiwan). HEK293T cells and NCCIT cells were maintained in Dulbecco's modified Eagle's medium and Roswell Park Memorial Institute 1640 medium, each supplemented with 10% fetal bovine serum

(all Gibco/Life Technologies). These cells were incubated at 37°C in a humidified atmosphere of 5% CO_2.

Methylated and Hydroxymethylated DNA Immunoprecipitation Analysis

Total DNA was extracted from biological samples and sequenced using the Illumina Hiseq2000 and Nextseq system according to the manufacturer's instructions. Briefly, double-strand DNA was sonicated and then ligated to adaptor for further amplification (Qiagen GeneRead Library Prep). Next, the double-strand DNA was denatured and immunoprecipitated with anti–5'-methylcytosine and anti–5'-hydroxymethylcytosine antibodies (1 μg, Active Motif), respectively, overnight. The enriched methylated DNA fragment was amplified by polymerase chain reaction (PCR) (GeneRead DNA I Amp Kit), and high-throughput sequencing was performed.

Filtered reads were first mapped using Hg19 as the reference. To identify differential methylation and hydroxymethylation regions (DMRs and DhMRs), bam format files were used as input for the MEDIPS algorithm.[15] The window of each DMR was set to 250 bps, and the minimum number of reads for each group was set to 10. The identified regions of DMRs and DhMRs in NGMGCTs were compared with germinomas. DMRs and DhMRs were considered significant when $P < 0.05$ and < 0.01, respectively. DMRs and DhMRs were annotated according to their genomic location by using ChIPseeker, an R package.[16]

Small RNA Sequencing Analysis

Total RNA was collected, and small RNA fractions were sequenced using an Illumina HiSeq 2000 and Nextseq, according to the manufacturer's instructions. Briefly, total RNA was subjected to directional RNA adapter ligation, first strand cDNA synthesis, and size selection. The cDNA corresponding to small RNA (16 to 30 nt) was collected and sequenced. Raw sequencing reads in the FASTQ format were generated and then subjected to our in-house bioinformatics pipelines for miRNA profiling and discovery.[17]

Lentivirus Production and Transduction

Knockdown or miRNA expression plasmids were co-transfected with 2 packaging plasmids, pCMV-dR8.91 and pMD2.G, into HEK293T cells by using the TurboFect transfection reagent (Thermo Scientific). The virus suspension was harvested by filtering the culture media through 0.22-μm filters (Nalgene) at 48 and 72 h after transfection. For lentivirus transduction, the virus suspension was added to NCCIT cells, and transduced cells were selected by the antibiotic resistance marker blasticidin (10 μg/mL) or puromycin (2 μg/mL) for 1 week. All procedures involving the manipulation of infectious materials were performed in a Biosafety Level 2 laboratory.

RNA and Reverse Transcription Quantitative PCR

Total RNAs of tumor tissues and cultured cells were isolated using TRIzol reagent (Invitrogen/Life Technologies).

Total RNA was reverse-transcribed (RT) into complementary DNA through miRNA-specific or random hexamer priming using a RevertAid First Strand cDNA Synthesis Kit (Thermo Scientific). MiRNA-specific and U6-specific RT primers are shown in Supplementary Table S1. Quantitative PCR was performed in duplicate with miRNA- or gene-specific primers by using a Maxima SYBR FAST quantitative (q)PCR kit (Thermo Scientific), and the specific product was detected and analyzed using the StepOnePlus Real-Time PCR System. MiRNA-specific and U6-specific qPCR primers are shown in Supplementary Table S1. Quantitative PCR was performed in a 20-μL reaction volume consisting of 10 μL 2× SYBR green mix, 0.5 μL of 10 μM forward primer, 0.5 μL of 10 μM reverse primer, 8 μL nuclease-free water, and 1 μL template. For gene detection, thermal cycle was programmed for 10 minutes at 95°C as initial denaturation, followed by 40 cycles of 15 sec at 95°C for denaturation, 15 sec at 58°C for annealing, and 30 sec at 72°C for extension. For miRNA detection, thermal cycle was programmed for 5 minutes at 95°C as initial denaturation, followed by 40 cycles of 10 sec at 95°C for denaturation, and 60 sec at 60°C for annealing and extension. Relative gene expression changes were evaluated with the $2^{-\Delta\Delta C_T}$ method.[18] The cycle threshold (C_T) values of the target genes or miRNAs were subtracted to internal control glyceraldehyde 3-phosphate dehydrogenase or U6 expression levels, respectively, within the same sample to determine ΔC_T, and then average ΔC_T values of technical replicates were calculated. For each gene or miRNA of interest, the ΔC_T values of the testing group were then subtracted to the average ΔC_T of the control group to obtain $\Delta\Delta C_T$ The expression levels were presented as fold change using $2^{-\Delta\Delta C_T}$.

5-Aza-2′-Deoxycytidine Treatment

In the 5-aza-2'-deoxycytidine (Sigma) treatment, NCCIT cells were incubated with 2.5, 5, and 10 μM of 5-aza-2'-deoxycytidine or with a corresponding amount of dimethyl sulfoxide for 96 h. The medium was changed every 24 h. The cells were then harvested for RNA extraction.

MTT Assay and Cisplatin Treatment

To evaluate cell viability, cells were seeded at 1×10^4/well and incubated at 37°C. After incubation for 24 h, the cells were treated with different concentrations of cisplatin for 48 h. After 48 h, the cells were treated with 1% thiazolyl blue tetrazolium for 30 min at 37°C, followed by 0.1% sodium dodecyl sulfate in 2-propanol, and thorough mixing was performed. The results were obtained by measuring the absorbance at wavelengths of 570 and 650 nm using a multiwell scanning spectrophotometer.

Immunoblotting

Knockdown or miRNA expression plasmids were introduced into NCCIT cell lines using lentiviruses. After 48 h, the cells were harvested and lysed using NET lysis buffer containing protease and phosphatase inhibitors. Immunoblotting was performed using anti-BCL2L11 (1:1000; Cell Signaling) and

anti–caspase-3 (1:1000; Cell Signaling) antibodies, followed by visualization using horseradish peroxidase–conjugated secondary antibodies and an enhanced chemiluminescence detection system (Merck Millipore).

In Vitro Methylation and Reporter Assay

In brief, 1 μg of the purified plasmid DNA was incubated with the cytosine-phosphate-guanine (CpG) methyltransferase M.SssI (New England Biolabs) and S-adenosylmethionine at 37°C for 1 h. The methylated plasmids were extracted by using PCR cleanup kits (Bioman). The protein expression plasmid (600 ng), methylated plasmid (300 ng), and Renilla luciferase plasmid (15 ng) were co-transfected into 1.5×10^5 HEK293T cells by using the TurboFect transfection reagent. Luciferase activity was measured using a luminometer (model LB593, Berthod). Firefly luciferase activity was normalized to Renilla luciferase activity.

Immunohistochemistry

Immunohistochemistry (IHC) sample preparation and staining were performed as described previously.[19] The antibodies used were anti-BCL2L11 (1:100) and anti–BCL-XL (1:1000; Cell Signaling).

Statistics Analysis

Independent sample *t*-tests were performed to compare the continuous variation between the 2 groups. $P < 0.05$ was considered significant. All data are reported as mean ± SD.

Results

Distribution of DMRs and DhMRs and Identifying Methylation-Regulated mRNAs

MeDIP- and hMeDIP-seq were performed to examine the differential distribution of 5mC and 5hmC between germinomas and NGMGCTs. Our study included 6 germinomas and 6 NGMGCTs; the supporting clinical information is listed in Table 1. Regions that showed significant changes in the 5mC and 5hmC methylation in NGMGCTs compared with germinomas are defined as DMRs and DhMRs, respectively. Both 5mC and 5hmC modifications were widely distributed across the genome, and the DMRs and DhMRs occurred more frequently at introns and distal intergenic regions (Fig. 1A). Occurrence of DMRs at promoter region was about 11% (NGMGCT hypomethylation) and 10% (NGMGCT hypermethylation); DhMRs at promoter region were about 4.5% (NGMGCT hypohydroxymethylation) and 14% (NGMGCT hyperhydroxymethylation). Gene expression was associated with the presence of higher 5hmC and lower 5mC at the gene promoter regions. Furthermore, non-CpG island promoter methylation silences gene expression.[20] To determine genes regulated through methylation, genes with DMRs and DhMRs

occurring at the promoter region were selected and their gene expression values were obtained from our previously published mRNA microarray dataset.[13] We identified 26 downregulated genes that had higher promoter 5mC and lower 5hmC and 71 upregulated genes that had lower promoter 5mC and higher 5hmC in NGMGCTs compared with germinomas (Fig. 1B and C). The top 10 upregulated and downregulated genes are listed in Supplementary Table S2.

Small RNA Sequencing Reveals Differential Expression of Known and Novel MiRNAs

To identify the miRNome differences between germinomas and NGMGCTs, the global miRNA expression patterns of 6 germinomas and 7 NGMGCTs were investigated using small RNA sequencing (smRNA-seq) and analyzed with our in-house bioinformatics pipelines.[21] In addition to known miRNAs, novel miRNA candidates were predicted using 3 independent bioinformatics algorithms (miRDeep2, mireap, and miRanalyzer) after removal of mRNA contamination and known miRNAs. In total, we identified 159 known and 27 novel miRNAs differentially expressed between germinomas and NGMGCTs ($q < 0.01$; Fig. 2A and Supplementary Figure S1A). The top 20 upregulated and downregulated miRNAs are listed in Table 2, and the other significant known miRNAs are listed in Supplementary Table S3. Through RNA fold analysis (http://rna.tbi.univie.ac.at/cgi-bin/RNAfold.cgi), we verified that these novel miRNA candidates can fold into a hairpin secondary structure (Supplementary Figure S1B); all the differentially expressed novel miRNA candidates are listed in Supplementary Table S4.

Identifying Epigenetically Regulated miRNAs in Germinomas and NGMGCTs

To decipher methylation-regulated miRNAs, we first determined the miRNA transcription start site by using miRStart (http://mirstart.mbc.nctu.edu.tw/browse.php) and selected miRNAs with DMRs and DhMRs occurring at the promoter region. By comparing the expression of the selected miRNAs using the smRNA-seq dataset, we identified 2 downregulated (miR-142-5p and miR-142-3p) and 6 upregulated miRNAs (miR-199a-3p, miR-199a-5p, miR-214-3p, miR-214-5p, miR-218-5p, and miR-585-3p) in NGMGCTs that might be under methylation-dependent transcriptional regulation (Fig. 2B). The miR-214/199a cluster contains 4 genes (miR-214-3p, miR-214-5p, miR-199a-3p, and miR-199a-5p) and its promoter DMRs and DhMRs are located at chr1:172,114,251–172,114,750 and chr1:172,116,251–172,117,000, respectively (Supplementary Figure S2A). MiRNAs within this cluster were found to be upregulated in NGMGCTs. We validated the expression levels of miR-214-3p and miR-199a-5p using reverse transcription quantitative PCR (RT-qPCR), and the PCR data correlated well with the sequencing results (Fig. 2C). Furthermore, the reads per million of miR-214-3p and miR-199a-5p were negatively correlated with their methylation status (correlation = –0.8458 and –0.7454, respectively; Fig. 2D). NCCIT

Table 1 Clinical details of sequencing patients enrolled in MeDIP-seq, hMeDIP-seq, small RNA-seq, and mRNA array

Sample No.	Age, y	Sex	Pathological Diagnosis	Surgical Excision	Treatment	AFP	HCG	MeDIP-seq	hMeDIP-seq	smRNA-seq	mRNA Array
G1	14.1	M	G	STR	RT	N	N	+	+	+	+
G2	11.6	M	G	PR	RT	N	N	+	+	−	+
G3	13.9	M	G	NTR	RT	N	N	+	+	+	−
G4	14.0	M	G	PR	RT+CMT	H	N	+	+	+	+
G5	11.4	F	G	PR	RT	N	N	+	+	+	−
G6	12.4	M	G	PR	RT	N	N	+	+	+	−
G7	16.0	M	G	STR	RT	N	N	−	−	+	+
G8	12.2	M	G	PR	RT	N	N	−	−	−	+
G9	10.4	F	G	PR	RT	N	N	−	−	−	+
NG1	11.5	M	MGCT (G+IT+YSC)	STR	RT+CMT	H	N	+	+	+	−
NG2	4.3	M	MGCT (G+IT)	NTR		N	N	+	−	−	+
NG3	0.7	M	IT	NTR	RT+CMT	H	N	+	+	+	−
NG4	14.5	M	MGCT (G+YSC)	PR	RT+CMT	H	N	+	+	+	+
NG5	7.6	M	MGCT (EC+IT+YSC)	NTR	RT+CMT	H	H	+	+	+	+
NG6	10.3	M	MGCT (IT+G)	NTR	RT+CMT	N	N	+	+	+	+
NG7	0.0	F	IT	NTR		H	N	−	+	+	+
NG8	0.1	F	IT	NTR	RT+CMT	H	N	−	−	+	−
NG9	10.6	M	MGCT (IT+YSC)	PR	RT+CMT	H	H	−	−	−	+

Abbreviations: G, germinoma; NTR, near total removal, >95%; MGCT, mixed GCT; STR, subtotal removal, >75%; IT, immature teratoma; PR, partial removal, >25% <75%; YSC, yolk sac tumor; RT, radiotherapy; CMT. chemotherapy; normal range of AFP <10 ng/dL; EC, embryonal carcinoma; normal range of betaHCG <10 mIU/dL; "+": sequenced; "−": not sequenced; NG, NGMGCTs or nongerminomatous malignant germ cell tumors; N, normal level; H, high level.

is an embryonal carcinoma cell line and its expression pattern was positively correlated with intracranial germ cell tumors (Pearson correlation coefficient r = 0.8–0.9; Supplementary Figure S2B). The miR-214/199a promoter showed higher 5mC methylation and lower 5hmC methylation, which was similar to the pattern of germinomas (Supplementary Figure S2A). Therefore, we treated NCCIT cells with different concentrations of 5′-aza for 96 h and both miR-214-3p and miR-199a-5p were upregulated after 5′-aza treatment (Fig. 2E). Bisulfite sequencing confirmed demethylation of the miR-214/199a promoter after 5′Aza treatment (Supplementary Figure S2C). Gene promoter methylation inhibits transcription through 2 basic mechanisms: (i) modification of CpG sites within transcription factor binding sites, and (ii) specific binding of methyl-CpG-binding domain proteins to methylated CpG sites to indirectly affect transcription factor binding.[22] To determine whether CpG methylation status in the DMRs of the miR-214/199a promoter affects miR-214 and miR-199a expression, we conducted in vitro methylation assays using luciferase reporters containing the full-length miR-214/199a minimal promoters. The cloned

sequence and plasmid map are shown in Supplementary Figure S3. CpGs in the promoter region were methylated in vitro using CpG methyltransferase M.SssI before transfection into 293T cells for the luciferase reporter assay. The promoter activity of the miR-214/199a cluster was reduced upon CpG methylation by M.SssI (Fig. 2F). Next, we wish to determine if miR-214/199a promoter methylation affects transcription factor–dependent expression. The Twist1 and Twist2 transcription factors were upregulated in NGMGCTs (Supplementary Figure S4), therefore we co-transfected 293T cells with methylated miR-214/199a promoter reporter plasmids and Twist expression plasmids (Twist1 and Twist2) to detect luciferase activity. Twist proteins have been demonstrated to regulate miR-214/199a expression by binding to E-box elements in the promoter region.[23,24] We found that the Twist-binding site does not contain CpG sites; the expression of Twist1 and Twist2 should enhance the luciferase activity of the miR-214/199a promoter reporter plasmid. However, the luciferase activity was reduced when the miR-214/199a promoter reporter plasmid was methylated (Fig. 2F). These data suggested that miR-214/199a
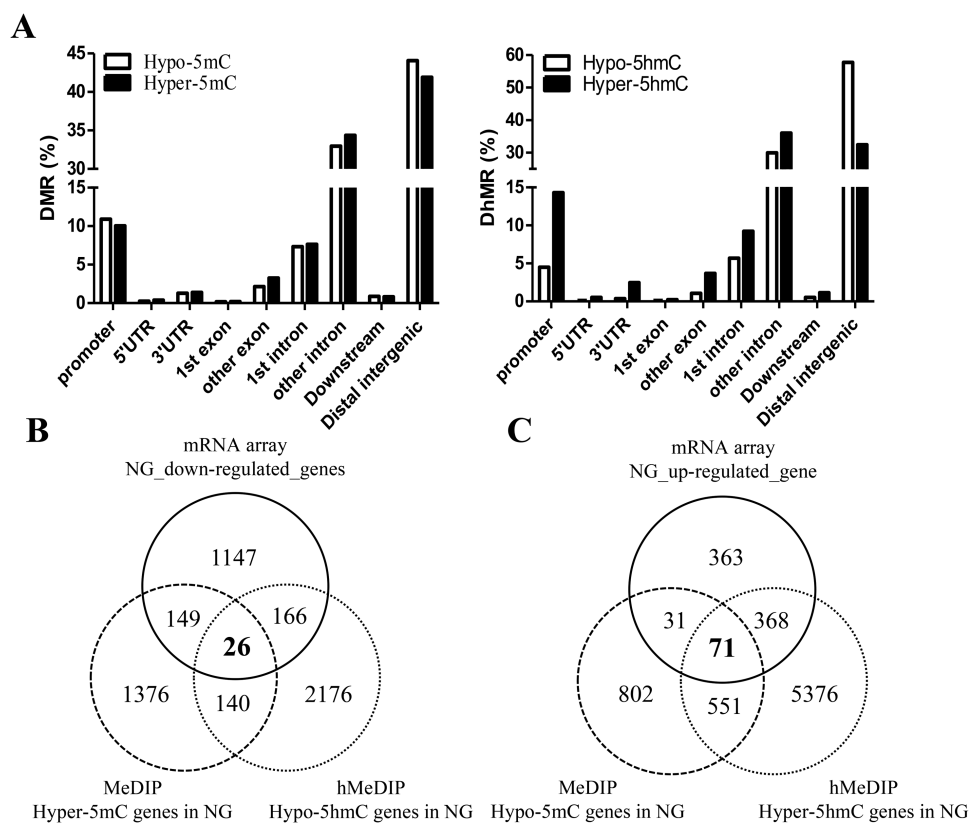
Fig. 1 Identification of methylation-regulated mRNAs between germinomas and NGMGCTs. (A) Distribution of DMRs (left) and DhMRs (right) within genomic regions. (B–C) Venn diagram demonstrating the principle of putative methylation- and hydroxymethylation-regulated mRNAs. The number of intersections indicates the overlapped mRNAs across each group. (B) Comparison of downregulated, hypermethylated, and hypohydroxymethylated genes in NGMGCTs. (C) Comparison of upregulated, hypomethylated, and hyperhydroxymethylated genes in NGMGCTs.

promoter methylation affects transcription factor–dependent miRNA expression.

MiR-214-3p Overexpression Leads to Cisplatin Resistance Through Downregulation of BCL2L11

Previous studies showed that aberrant miRNA expression was associated with chemotherapy resistance by targeting apoptosis-related genes. For example, overexpression of MET protein resulted in tyrosine kinase inhibitor resistance in lung cancers. Garofalo et al demonstrated that MET could induce miR-221/222 and miR-30b/c expression, which in turn targeted the pro-apoptotic proteins apoptotic protease activating factor 1 (APAF-1) and BIM. They showed that overexpression of miR-221/222 and miR-30b/c in HCC827 and PC9 cells significantly reduced gefitinib-induced cell death. They co-transfected wild-type or mutated miRNA binding sites of BIM and APAF-1–containing expression vectors with miR-221/222 and miR-30b/c expression vectors and performed caspase-3/7 and viability assays. They observed increased caspase-3/7 activity when cells were co-transfected with APAF-1 and BIM containing mutated miRNA binding sites and miR-NAs. These data suggested that the effects of apoptotic

proteins on chemotherapy resistance were directly related to miRNA expression.[25] We showed methylation-dependent upregulation of miR-214/199a expression in NGMGCTs. Furthermore, miR-214-3p has been associated with cisplatin resistance in ovarian cancer[26] and tongue squamous cell carcinomas.[27] To identify whether miR-214-3p is involved in cisplatin resistance in NGMGCTs, we first determined the half-maximal inhibitory concentration values of cisplatin in NCCIT cells to be 6.52 μM (Supplementary Figure S5). Next, we stably expressed miR-214-3p in NCCIT cells (Fig. 3A) and monitored the corresponding cell viability after treatment with different concentrations of cisplatin and etoposide. NCCIT-miR-214-3p cells showed significant resistance to cisplatin cytotoxicity compared with NCCIT-vector cells (Fig. 3B). However, no difference was observed in the survival rates between the NCCIT-miR-214-3p and NCCIT-vector cells treated with etoposide (data not shown). To determine whether miR-214-3p enhances chemotherapy resistance through the regulation of cell proliferation, we seeded cells and assessed the proliferation rate through MTT assay at days 0, 1, 3, 5, and 7. Both NCCIT-miR-214-3p and NCCIT-vector cells had similar proliferation rates (Supplementary Figure S6), which suggests that cisplatin resistance mediated by miR-214-3p does not involve cell proliferation.
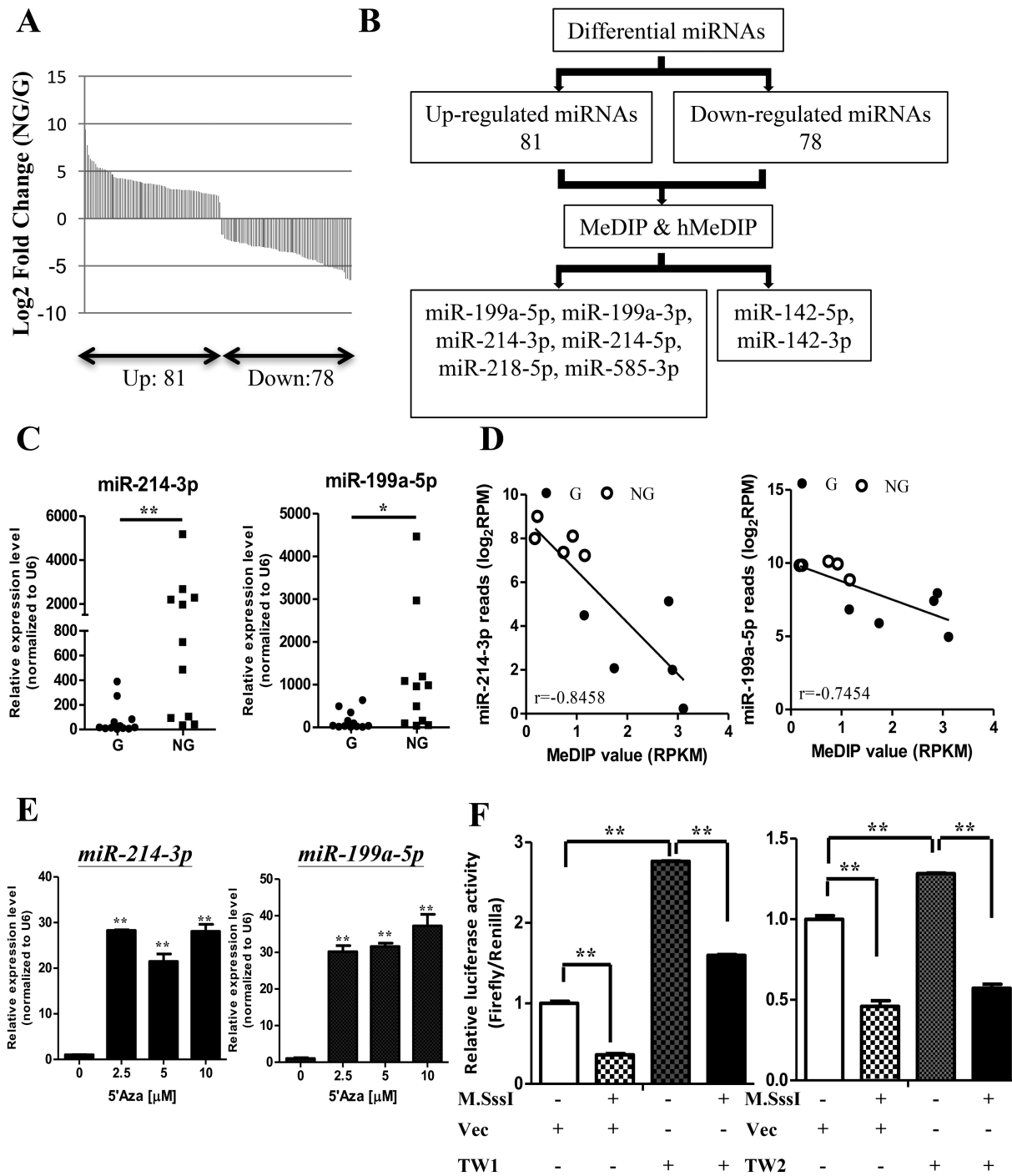
Fig. 2 Identification of methylation-regulated miRNAs and miR-199a/214 cluster expression regulated through DNA methylation. (A) Small RNA-Seq revealed differentially expressed known miRNAs between germinomas and NGGCTs ($q < 0.01$). (B) Schematic representation for identifying methylation-regulated miRNAs. The putative targets were obtained by overlapping the differentially expressed miRNAs and differentially methyl-ated miRNA promoter region identified from MeDIP and hMeDIP-sequencing. A total of 8 miRNA expressions might be regulated by methylation (6 upregulated and 2 downregulated in NGMGCTs). (C) MiR-214-3p (left) and miR-199a-5p (right) were upregulated in NGMGCTs ($n = 11$) com-pared with germinomas ($n = 12$) (*$P < 0.05$, **$P < 0.01$, by t-test). (D) Scatter plots illustrating negative correlations between MeDIP values and the reads per million of miR-214-3p (left) and miR-199a-5p (right). Every dot denotes one sample in which MeDIP-seq and smRNA-seq were both performed. (E) Expression of miR-214-3p (left) and miR-199a-5p (right) after treatment with different concentrations of 5-aza-2′-deoxycytidine (2.5, 5, and 10 μM). Expression values expressed as mean ± SD in duplicates and representative of 3 independent experiments. (F) Constructs of the miR-199/214 promoter (length: 1000 bps) that was methylated with M.SssI in vitro and co-transfected with Twist1 (left) and Twist2 (right) expression vectors into 293T cells. Luciferase activities of the methylated expression vectors were normalized to the expression of Renilla firefly luciferase and are representative of 3 independent experiments (**$P < 0.01$, by t-test).

Table 2 Small RNA-sequencing showed 81 upregulated and 78 downregulated miRNAs (top 20 differential miRNAs [left: upregulated; right: downregulated])

Name	Average RPM (G)	Average RPM (NG)	LogFC (NG/G)	Name	Average RPM (G)	Average RPM (NG)	LogFC (NG/G)
hsa-miR-675-5p	0.00	18.63	∞	hsa-miR-520a-5p	20.04	0.14	−7.15
hsa-miR-122-5p	1.61	9179.46	12.48	hsa-miR-520f-3p	164.30	1.23	−7.06
hsa-miR-206	5.07	5796.09	10.16	hsa-miR-520b	95.75	0.76	−6.97
hsa-miR-194-3p	0.06	32.15	9.15	hsa-miR-520c-3p	82.19	0.67	−6.94
hsa-miR-585-3p	0.11	49.72	8.78	hsa-miR-515-3p	5.40	0.05	−6.87
hsa-miR-203b-3p	0.04	13.51	8.48	hsa-miR-526b-3p	17.91	0.25	−6.16
hsa-miR-490-5p	0.08	21.22	8.13	hsa-miR-516b-3p	38.98	0.68	−5.85
hsa-miR-203a-3p	9.80	2275.29	7.86	hsa-miR-516a-3p	38.98	0.68	−5.85
hsa-miR-196a-5p	6.47	1348.96	7.70	hsa-miR-520e	13.61	0.24	−5.81
hsa-miR-135a-3p	0.72	134.85	7.55	hsa-miR-150-5p	1671.90	31.56	−5.73
hsa-miR-196b-5p	5.35	949.85	7.47	hsa-miR-3614-5p	4.11	0.10	−5.36
hsa-miR-675-3p	0.78	135.87	7.45	hsa-miR-5701	52.75	1.54	−5.10
hsa-miR-200b-5p	0.32	39.08	6.93	hsa-miR-96-3p	6.91	0.20	−5.10
hsa-miR-1262	0.28	30.73	6.76	hsa-miR-548x-3p	7.50	0.24	−4.97
hsa-miR-323b-3p	0.38	40.32	6.72	hsa-miR-202-5p	2.64	0.09	−4.89
hsa-miR-375	7.48	657.19	6.46	hsa-miR-3180-5p	3.89	0.14	−4.84
hsa-miR-216b-5p	2.02	167.70	6.38	hsa-miR-548aj-3p	10.27	0.39	−4.70
hsa-miR-1-3p	70.71	5608.09	6.31	hsa-miR-6502-5p	1.75	0.07	−4.62
hsa-miR-487a-5p	0.19	12.97	6.10	hsa-miR-422a	42.78	1.75	−4.62
hsa-miR-449b-5p	1.38	94.52	6.09	hsa-miR-548ae-3p	10.24	0.45	−4.52
G: Germinomas	NG: NGMGCTs						

Abbreviations: RPM, reads per million; G, germinoma; NG, NGMGCTs or nongerminomatous malignant germ cell tumors.

Next, we used Targetscan (http://www.targetscan.org/) to identify which expressed genes were direct targets of miR-214-3p, and we compared these results with the downregulated genes in NGMGCTs. We determined that miR-214-3p potentially targeted 314 genes, among which 4 were apoptosis-related genes localized in the mitochondria (Fig. 3C). BCL2L11, also known as BIM, is a proapoptotic protein.[28] BCL2L11 was shown to be the direct target of miR-214-3p.[29] In our study, miR-214-3p overexpression reduced BCL2L11 mRNA and protein expression (Fig. 3D). Knockdown of BCL2L11 resulted in increased cisplatin resistance compared with control cells (NCCIT-shvec; Fig. 3E). BCL2L11 knocked-down cells produced an additional cleaved form of caspase-3 after cisplatin treatment (Fig. 3F). These results demonstrate that BCL2L11 is the direct target of miR-214-3p, and the loss of BCL2L11

expression inactivates the apoptosis pathway and confers cisplatin resistance.

Expression of BCL2L11 Was Downregulated in NGMGCTs

We validated BCL2L11 expression in our clinical samples and determined that out of 12 cases of germinomas, 7 (60%) showed upregulated BCL2L11 expression and 5 showed similar or downregulated BCL2L11 expression, compared with NGMGCTs (Fig. 4A). IHC staining indicated that germinomas had strong and intermediate BCL2L11 immunoreactivity (Fig. 4B and C), whereas NGMGCTs had weaker positivity for BCL2L11 (Fig. 4D–F). IHC assessment of another important apoptotic factor, BCL-XL, showed that both types of GCTs had similar staining intensities.
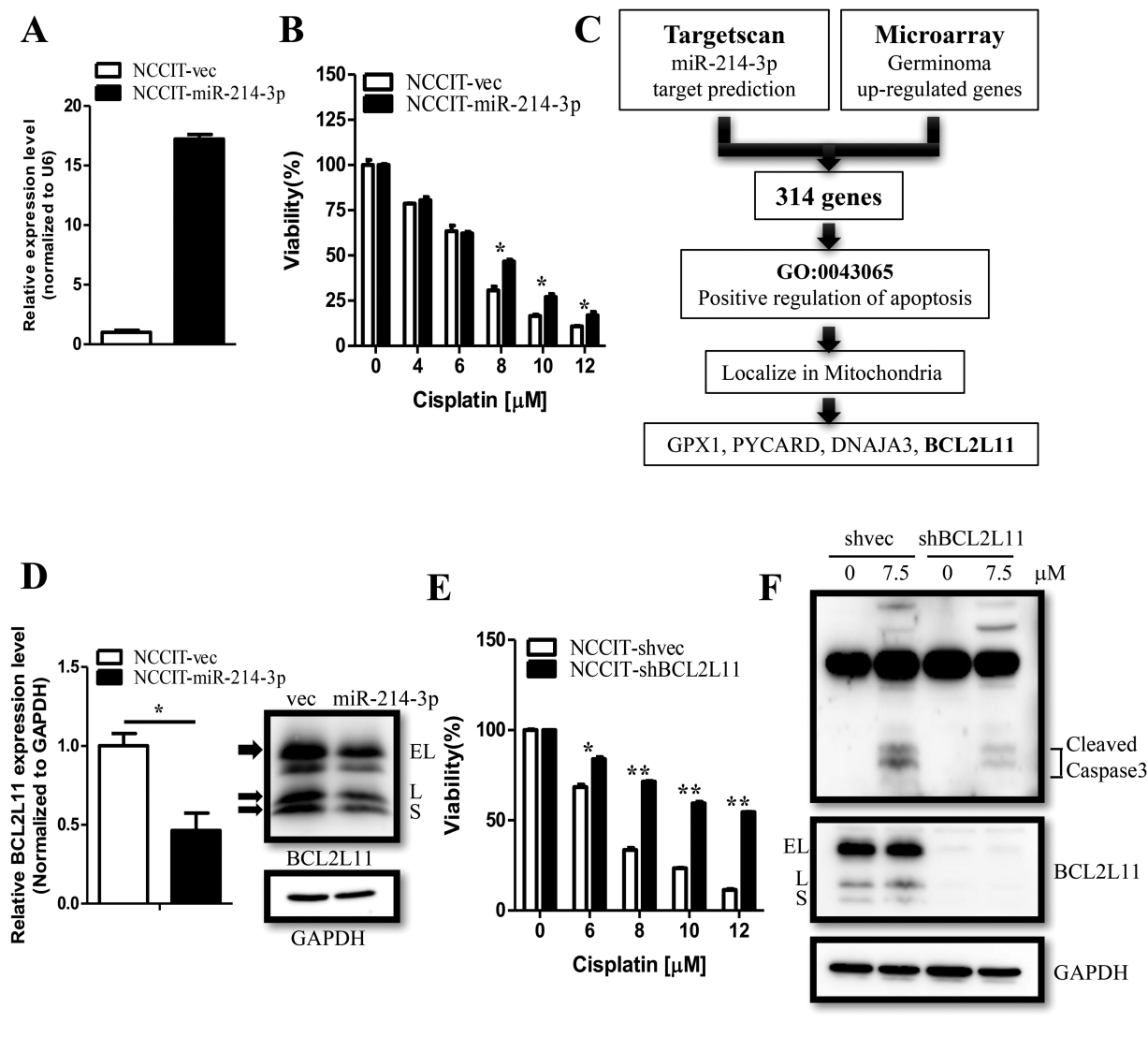
Fig. 3 MiR-214-3p enhanced cisplatin resistance by targeting the pro-apoptotic protein BCL2L11. (A) Overexpression of miR-214-3p in NCCIT cells confirmed with RT-qPCR. (B) NCCIT-vector cells and NCCIT-miR-214-3p cells were treated with cisplatin at different concentrations (4, 6, 8, 10, and 12 µM). Cell viability was detected through MTT assay. Viabilities are expressed as mean ± SD from duplicate wells and are representative of 3 independent experiments (*$P < 0.05$, by t-test). (C) Schematic representation for identifying miR-214-3p targets. The putative targets were obtained by overlapping the downregulated genes in NGMGCTs and the software-predicted targets. The target genes that we were interested in, that is, the apoptotic genes, were localized in the mitochondria. Four genes were listed. (D) Immunoblotting (right) and RT-qPCR (left) confirmed the levels of BCL2L11 in NCCIT-miR-214-3p cells. RT-qPCR data are shown as mean ± SD in duplicates, and immunoblotting and RT-qPCR are representative of 3 independent experiments. (E) BCL2L11 knocked-down (KD) cells were treated with cisplatin at different concentrations (6, 8, 10, and 12 µM). Cell viability was detected through MTT assay. Viabilities are expressed as mean ± SD from duplicate wells and are representative of 3 independent experiments (**$P < 0.01$, *$P < 0.05$, by t-test). (F) BCL2L11-KD cells were treated with 7.5 µM cisplatin, and the levels of caspase-3 were detected through immunoblotting.

Discussion

Clinical treatments of NGMGCTs include surgery and a combination of standard dose radiotherapy and intensive chemotherapy. However, the overall survival of NGMGCTs is still markedly lower than that in germinomas.[13] Previous studies demonstrated that treatment with DNA demethylating agent 5′-aza changed the methylation patterns of radiation-resistant

and chemoresistant cells, and restored the chemo- and radiotherapy sensitivity of these cells.[28,29] The results suggest that one of the mechanisms for tumor cell resistance to chemo- and radiotherapy is change in DNA methylation patterns to affect gene expression.[30,31] DNA mutation or aberrant expression of components and cofactors involved in the epigenetic modification and its regulation has been observed in tumors.[32,33] Rare germline variants have been found in histone demethylase, Jumonji domain containing
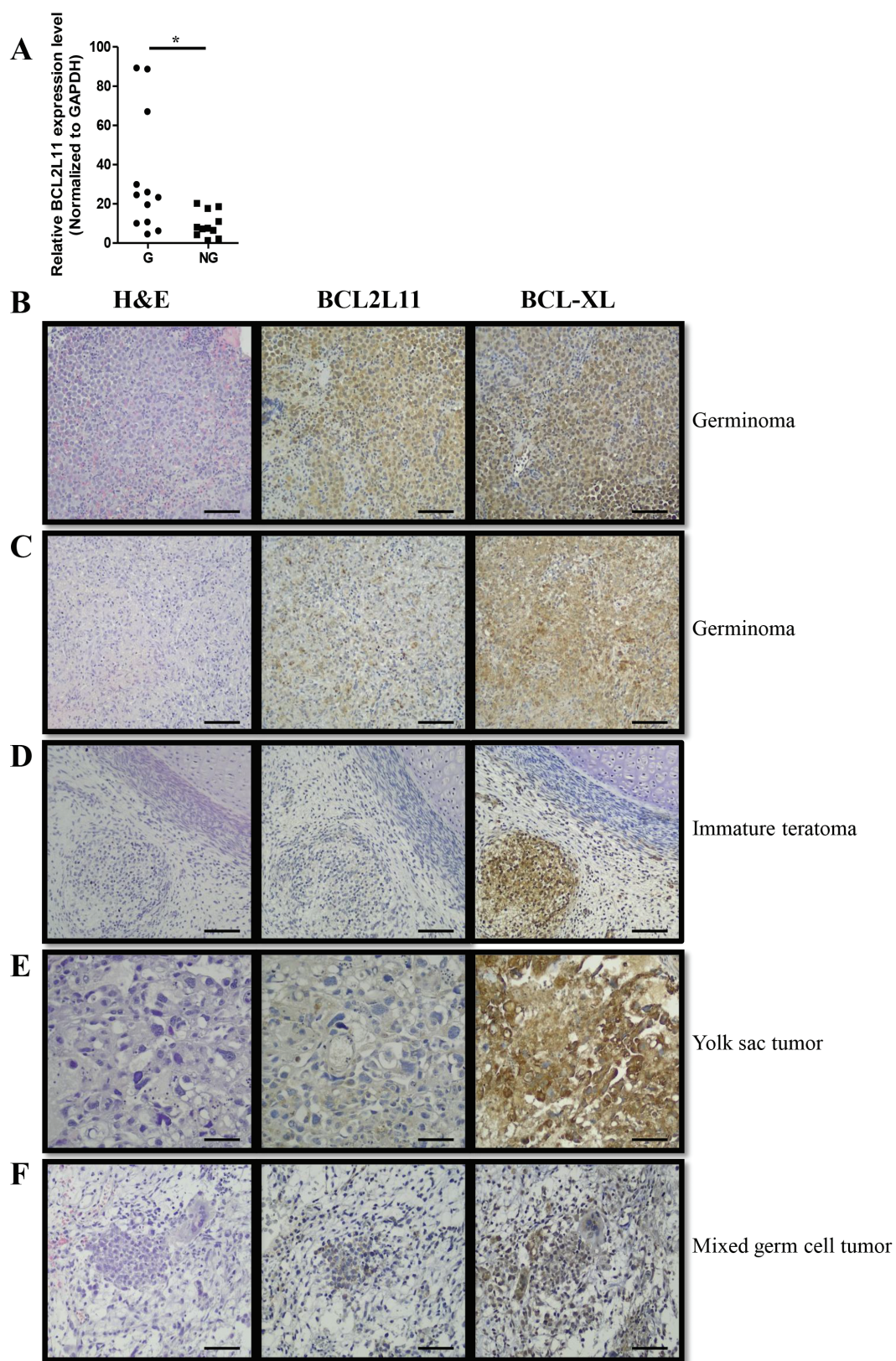
Fig. 4 BCL2L11 expression was downregulated in NGMGCTs. (A) RT-qPCR confirmed lower mRNA levels of BCL2L11 in NGMGCTs ($n = 11$) than in germinomas ($n = 12$) (**$P < 0.01$, by t-test). (B–F) IHC results for hematoxylin and eosin staining of BCL2L11 and BCL-XL in germinoma and NGMGCT specimens. (B–C) Germinomas. (D) Immature teratoma. (E) Yolk sac tumor. (F) Mixed germ cell tumors. Scale bar: 100 μm.

1C (*JMJD1C*) in Japanese intracranial GCT patients.[34–36] However, genes encoding for the major methylation-regulating enzymes, including *DNMT1, DNMT3A, DNMT3B, TET1, TET2,* and *TET3*, were not mutated in CNSGCTs. Also, our data showed that the *TET1* gene was slightly upregulated in germinomas,[13] whereas other DNA methylation–associated genes had no significant difference in expression compared with NGMGCTs. Therefore, the mechanism for the differential 5mC and 5hmC patterns between germinomas and NGMGCTs still remains to be elucidated.

Cisplatin has been used to treat several types of cancers. However, many solid tumors can easily acquire cisplatin resistance, thus limiting its therapeutic efficacy. Several mechanisms have been proposed that contribute to cisplatin resistance in various cancers, including (i) reduced cisplatin accumulation by regulating drug transport and uptake, (ii) increased levels of glutathione, glutathione-S-transferase, or metallothioneins to detoxify cisplatin, (iii) altered DNA repair involving loss of mismatch repair or increased nucleotide excision repair, (iv) altered DNA damage tolerance, and (v) reduced apoptosis induction.[37] The pro-apoptotic protein BCL2L11 (BIM) is associated with cisplatin resistance in several cancers, including ovarian cancer[38] and hepatocarcinoma.[39] Furthermore, better prognosis correlates with higher BCL2L11 expression in nasopharyngeal carcinomas.[29]

Dysregulated miRNA expression is well known in cancers and can contribute to chemotherapy resistance through the binding and transcription regulation of downstream targets.[40] In the present study, 159 miRNAs were differentially expressed in NGMGCTs compared with germinomas, and several miRNAs have been reported to regulate cisplatin sensitivity in other cancers. Previously, miR-449a was reported to regulate cisplatin sensitivity by targeting BCL2 expression in the gastric cancer cell line SGC7901.[41] In addition, miR-214 overexpression has been shown to target phosphatase and tensin homolog gene expression to affect cell survival and cause cisplatin resistance in ovarian cancers.[26] In our study, we showed that miR-214-3p overexpression contributed to cisplatin resistance in NGMGCTs by inhibiting BCL2L11 expression, whereas there is no significant difference in expression of phosphatase and tensin homolog between germinomas and NGMGCTs. In nasopharyngeal carcinoma cells, *BCL2L11* expression is regulated by miR-214 and miR-214 silencing, resulting in cell apoptosis and suppression of cell proliferation and tumor growth. Since germinomas and NCCIT cells showed low miR-214-3p expression, we treated cisplatin in miR-214-3p overexpressing NCCIT cells and observed significantly reduced cell death. In addition to its biological significance, miR-214-3p can serve as a plasma biomarker. Li D et al reported that the secretion of miR-214-3p–containing exosomes from osteoclast inhibits osteoblast activity and osteoblastic bone formation.[42] Hao M et al showed that a high level of serum miR-214 expression was associated with bone disease and poor prognosis in patients with multiple myelomas.[43] The level of miR-214-3p in the CSF and serum of NGMGCT patients remains to be determined. Moreover, Kuninty PR et al demonstrated that miR-214-3p and miR-199a-3p inhibition can downregulate cell proliferation, differentiation, and migration in cancer-associated fibroblasts in pancreatic tumor stroma.[44] Therefore, these findings suggest that miR-214 serves as a potential therapeutic candidate and biomarker for NGMGCT treatment.

In summary, integrative analysis of DNA methylome, transcriptome, and miRNome uncovered important differences in the epigenetic and miRNA-mediated transcriptional regulation between germinomas and NGMGCTs. Several methylation-regulated genes and miRNAs, specifically miR-214-3p, are hypomethylated and upregulated in NGMGCTs compared with germinomas. Our study determined that miR-214-3p expression contributed to cisplatin resistance by targeting the pro-apoptotic protein BCL2L11. The CNSGCT omics data from this study are a valuable resource that provides insight into the mechanisms of treatment resistance and could aid in the development of new antitumor therapeutic strategies.

Supplementary Material

Supplementary material is available at *Neuro-Oncology* online.

Conflict of interest statement. None declared.

References

1. Packer RJ, Cohen BH, Cooney K, Coney K. Intracranial germ cell tumors. *Oncologist*. 2000;5(4):312–320.
2. Wong TT, Ho DM, Chang KP, et al. Primary pediatric brain tumors: statistics of Taipei VGH, Taiwan (1975–2004). *Cancer*. 2005;104(10):2156–2167.
3. Matsutani M, Sano K, Takakura K, et al. Primary intracranial germ cell tumors: a clinical analysis of 153 histologically verified cases. *J Neurosurg*. 1997;86(3):446–455.
4. Huang PI, Chen YW, Wong TT, et al. Extended focal radiotherapy of 30 Gy alone for intracranial synchronous bifocal germinoma: a single institute experience. *Childs Nerv Syst*. 2008;24(11):1315–1321.

5. Lai IC, Wong TT, Shiau CY, et al. Treatment results and prognostic factors for intracranial nongerminomatous germ cell tumors: single institute experience. *Childs Nerv Syst*. 2015;31(5):683–691.

6. Robertson KD. DNA methylation and human disease. *Nat Rev Genet*. 2005;6(8):597–610.

7. Kriaucionis S, Heintz N. The nuclear DNA base 5-hydroxymethyl-cytosine is present in Purkinje neurons and the brain. *Science*. 2009;324(5929):929–930.

8. Rodríguez-Paredes M, Esteller M. Cancer epigenetics reaches mainstream oncology. *Nat Med*. 2011;17(3):330–339.

9. Pfeifer GP, Kadam S, Jin SG. 5-hydroxymethylcytosine and its potential roles in development and cancer. *Epigenetics Chromatin*. 2013;6(1):10.

10. Esteller M. Epigenetic gene silencing in cancer: the DNA hypermethylome. *Hum Mol Genet*. 2007;16 Spec No 1:R50–R59.

11. Wilting RH, Dannenberg JH. Epigenetic mechanisms in tumorigenesis, tumor cell heterogeneity and drug resistance. *Drug Resist Updat*. 2012;15(1-2):21–38.

12. Schickel R, Boyerinas B, Park SM, Peter ME. MicroRNAs: key players in the immune system, differentiation, tumorigenesis and cell death. *Oncogene*. 2008;27(45):5959–5974.

13. Wang HW, Wu YH, Hsieh JY, et al. Pediatric primary central nervous system germ cell tumors of different prognosis groups show characteristic miRNome traits and chromosome copy number variations. *BMC Genomics*. 2010;11:132.

14. Murray MJ, Saini HK, van Dongen S, et al. The two most common histological subtypes of malignant germ cell tumour are distinguished by global microRNA profiles, associated with differential transcription factor expression. *Mol Cancer*. 2010;9:290.

15. Lienhard M, Grimm C, Morkel M, Herwig R, Chavez L. MEDIPS: genome-wide differential coverage analysis of sequencing data derived from DNA enrichment experiments. *Bioinformatics*. 2014;30(2):284–286.

16. Yu G, Wang LG, He QY. ChIPseeker: an R/Bioconductor package for ChIP peak annotation, comparison and visualization. *Bioinformatics*. 2015;31(14):2382–2383.

17. Cheng WC, Chung IF, Huang TS, et al. YM500: a small RNA sequencing (smRNA-seq) database for microRNA research. *Nucleic Acids Res*. 2013;41(Database issue):D285–D294.

18. Livak KJ, Schmittgen TD. Analysis of relative gene expression data using real-time quantitative PCR and the 2(-Delta Delta C(T)) Method. *Methods*. 2001;25(4):402–408.

19. Ho DM, Shih CC, Liang ML, et al. Integrated genomics has identified a new AT/RT-like yet INI1-positive brain tumor subtype among primary pediatric embryonal tumors. *BMC Med Genomics*. 2015;8:32.

20. Han H, Cortez CC, Yang X, Nichols PW, Jones PA, Liang G. DNA methylation directly silences genes with non-CpG island promoters and establishes a nucleosome occupied promoter. *Hum Mol Genet*. 2011;20(22):4299–4310.

21. Cheng WC, Chung IF, Tsai CF, et al. YM500v2: a small RNA sequencing (smRNA-seq) database for human cancer miRNome research. *Nucleic Acids Res*. 2015;43(Database issue):D862–D867.

22. Pulido Fontes L, Quesada Jimenez P, Mendioroz Iriarte M. Epigenetics and epilepsy. *Neurologia*. 2015;30(2):111–118.

23. Yin G, Chen R, Alvero AB, et al. TWISTing stemness, inflammation and proliferation of epithelial ovarian cancer cells through MIR199A2/214. *Oncogene*. 2010;29(24):3545–3553.

24. Lee YB, Bantounas I, Lee DY, Phylactou L, Caldwell MA, Uney JB. Twist-1 regulates the miR-199a/214 cluster during development. *Nucleic Acids Res*. 2009;37(1):123–128.

25. Garofalo M, Romano G, Di Leva G, et al. EGFR and MET receptor tyrosine kinase-altered microRNA expression induces tumorigenesis and gefitinib resistance in lung cancers. *Nat Med*. 2011;18(1):74–82.

26. Yang H, Kong W, He L, et al. MicroRNA expression profiling in human ovarian cancer: miR-214 induces cell survival and cisplatin resistance by targeting PTEN. *Cancer Res*. 2008;68(2):425–433.

27. Yu ZW, Zhong LP, Ji T, Zhang P, Chen WT, Zhang CP. MicroRNAs contribute to the chemoresistance of cisplatin in tongue squamous cell carcinoma lines. *Oral Oncol*. 2010;46(4):317–322.

28. O'Connor L, Strasser A, O'Reilly LA, et al. Bim: a novel member of the Bcl-2 family that promotes apoptosis. *EMBO J*. 1998;17(2):384–395.

29. Zhang ZC, Li YY, Wang HY, et al. Knockdown of miR-214 promotes apoptosis and inhibits cell proliferation in nasopharyngeal carcinoma. *PLoS One*. 2014;9(1):e86149.

30. Ramachandran K, Speer C, Nathanson L, Claros M, Singal R. Role of DNA methylation in cabazitaxel resistance in prostate cancer. *Anticancer Res*. 2016;36(1):161–168.

31. Chen X, Liu L, Mims J, et al. Analysis of DNA methylation and gene expression in radiation-resistant head and neck tumors. *Epigenetics*. 2015;10(6):545–561.

32. Huang Y, Rao A. Connections between TET proteins and aberrant DNA modification in cancer. *Trends Genet*. 2014;30(10):464–474.

33. Ko M, An J, Pastor WA, Koralov SB, Rajewsky K, Rao A. TET proteins and 5-methylcytosine oxidation in hematological cancers. *Immunol Rev*. 2015;263(1):6–21.

34. Fukushima S, Otsuka A, Suzuki T, et al; Intracranial Germ Cell Tumor Genome Analysis Consortium (iGCT Consortium). Mutually exclusive mutations of KIT and RAS are associated with KIT mRNA expression and chromosomal instability in primary intracranial pure germinomas. *Acta Neuropathol*. 2014;127(6):911–925.

35. Wang L, Yamaguchi S, Burstein MD, et al. Novel somatic and germline mutations in intracranial germ cell tumours. *Nature*. 2014;511(7508):241–245.

36. Ichimura K, Fukushima S, Totoki Y, et al; Intracranial Germ Cell Tumor Genome Analysis Consortium. Recurrent neomorphic mutations of MTOR in central nervous system and testicular germ cell tumors may be targeted for therapy. *Acta Neuropathol*. 2016;131(6):889–901.

37. Köberle B, Tomicic MT, Usanova S, Kaina B. Cisplatin resistance: preclinical findings and clinical implications. *Biochim Biophys Acta*. 2010;1806(2):172–182.

38. Wang J, Zhou JY, Wu GS. Bim protein degradation contributes to cisplatin resistance. *J Biol Chem*. 2011;286(25):22384–22392.

39. Chi HC, Chen SL, Cheng YH, et al. Chemotherapy resistance and metastasis-promoting effects of thyroid hormone in hepatocarcinoma cells are mediated by suppression of FoxO1 and Bim pathway. *Cell Death Dis*. 2016;7(8):e2324.

40. Magee P, Shi L, Garofalo M. Role of microRNAs in chemoresistance. *Ann Transl Med*. 2015;3(21):332.

41. Hu J, Fang Y, Cao Y, Qin R, Chen Q. miR-449a Regulates proliferation and chemosensitivity to cisplatin by targeting cyclin D1 and BCL2 in SGC7901 cells. *Dig Dis Sci*. 2014;59(2):336–345.

42. Li D, Liu J, Guo B, et al. Osteoclast-derived exosomal miR-214-3p inhibits osteoblastic bone formation. *Nat Commun*. 2016;7:10872.

43. Hao M, Zang M, Zhao L, et al. Serum high expression of miR-214 and miR-135b as novel predictor for myeloma bone disease development and prognosis. *Oncotarget*. 2016;7(15):19589–19600.

44. Kuninty PR, Bojmar L, Tjomsland V, et al. MicroRNA-199a and -214 as potential therapeutic targets in pancreatic stellate cells in pancreatic tumor. *Oncotarget*. 2016;7(13):16396–16408.